



Institut für Numerische Simulation

Rheinische Friedrich-Wilhelms-Universität Bonn

Wegelerstraße 6 • 53115 Bonn • Germany
phone +49 228 73-3427 • fax +49 228 73-7527
www.ins.uni-bonn.de

Rodrigo Iza-Teran and Jochen Garcke

Operator Based Multi-Scale Analysis for Simulation Bundles

INS Preprint No. 1524

November 2015

Operator Based Multi-Scale Analysis of Simulation Bundles

Rodrigo Iza-Teran¹ and Jochen Garcke^{1,2}

¹Fraunhofer SCAI, Sankt Augustin

²Institut für Numerische Simulation, Universität Bonn

November 23, 2015

Abstract

We propose a new mathematical data analysis approach, which is based on the mathematical principle of symmetry, for the post-processing of bundles of finite element data from computer-aided engineering. Since all those numerical simulation data stem from the numerical solution of the same partial differential equation, there exists a set of transformations, albeit unknown, which map simulation to simulation. The transformations can be obtained indirectly by constructing a transformation invariant positive definitive operator valid for all simulations.

The eigenbasis of such an operator turns out to be a convenient basis for the handled simulation set due to two reasons. First, the spectral coefficients decay very fast, depending on the smoothness of the function being represented, and therefore a reduced multi-scale representation of all simulations can be obtained, which depends on the employed operator. Second, at each level of the eigendecomposition the eigenvectors can be seen to recover different independent variation modes like rotation, translation or local deformation. Furthermore, this representation enables the definition of a new distance measure between simulations using the spectral coefficients. From a theoretical point of view the space of simulations modulo a transformation group can be expressed conveniently using the operator eigenbasis as orbits in the quotient space with respect to a specific transformation group.

Based on this mathematical framework we study several examples. We show that for time dependent datasets from engineering simulations only a few spectral coefficients are necessary to describe the data variability, while the coarse variations get separated from the finer ones. Low dimensional structures are obtained in this way, which are able to capture information about the underlying simulation space. An effective mechanism to deal effectively with the analysis of many numerical simulations is obtained, due to the achieved dimensionality reduction.

1 Introduction

Computer-aided engineering (CAE) simulations are numerical solutions of partial differential equations (PDEs) which model the physical behavior of industrial products. Nowadays the art of simulation in industry is highly developed, large high performance computer systems are used to solve hundreds of finite element model variants. Engineers need to analyze and compare several thousand simulations in the product development process, with the goal to get the best product performance, while taking functional constraints, costs, or regulations into account.

The detailed analysis process usually involves evaluation of time dependent 3D animations of the product. Today in industry, a large amount of engineering know-how and time is invested for the evaluation of model variants based on the detailed investigation of the full results, e.g. in the form of movements or deformations, or the study of a few derived scalar quantities or performance curves. Analyzing and trying to identify cause and effect in the data set of computer simulations using the full finite element meshes in the range of millions of nodes is a challenging open problem. In this work, we introduce a novel analysis approach which can efficiently compare 3D finite element mesh data and therefore overcome this challenge.

The motivation and idea for our method come from principles that are used for the analytical solution of differential equations based on the notion of symmetry. Cartan's moving frame method [Car83] has inspired many analytical solution methods for differential equations and we also use its principles for our method. The proposed approach exploits a fundamental property of simulations, namely that they are solutions of partial differential equations. Therefore, simulations can be treated as mathematical objects which are symmetrical in the sense that one can apply a transformation to one, and that the new object after the transformation cannot be distinguished from the original one in the underlying mathematical space; in other words, it is invariant to the transformation. Finding such transformations can be very difficult and is problem dependent. Nevertheless we observe that such transformations, if available, are actually sending all simulations to an invariant space, so that instead of focusing on the transformation, we could instead focus on such space directly and try to find ways to obtain a representation of it. For certain practical situations this will be shown to be indeed possible.

As an example consider deformations of a car structure. In many practical cases, the changes between different simulations, e.g. due to variations in the material parameters, are distance preserving, that is after a deformation the distance between points in the structure are kept the same. In mathematical terms the transformation is therefore an isometry. Instead of looking for such a transformation directly, we here propose to look for some invariance property that is valid for all isometric changes, such property can be found in a differential operator. For this specific case, the Laplace-Beltrami operator, constructed using geodesic distances on the mesh, is an operator invariant to isometric transformations. If we assume that all simulations are obtained through such a transformation, the operator will be the same for all of them. Now, since this operator is positive semidefinite a spectral orthogonal decomposition can be found and an orthogonal basis of the invariant space can be constructed. In other words, an equivalent representation of the space, invariant to isometric changes, can be obtained. We now can project all simulations into this new basis in the form of their spectral coefficients and thereby obtain a set of equivalent, but transformed simulations, represented in the basis of the invariant space.

The number of basis elements in the new representation can be very large, in the order of the number of nodes in the discrete case. Nevertheless, we will see that under certain conditions, these coefficients decay very fast so that only few of them are big and reflect the variability of the simulations. This variability turns out to be captured in a multi-scale way, since the basis of the operator can separate geometrical coarse components from the finer ones. In summary, the original high dimensional simulations have been transformed into a compact multi-scale representation, enabling not only an efficient dimensionality reduction but also making further analysis tasks easier. Of course one can not assume that all simulations can be obtained as isometric transformations from a reference one and therefore we propose also a way, at least for certain type of problems, to generalize this approach using other types of operators. In particular we investigate one invariant to a general nonlinear transformation, the so-called nonlinear independent component analysis (NICA) operator.

We start with a summary of related research in section 2. The mathematical framework is presented in section 3, in particular we consider two types of invariant operators, the Laplace-

Beltrami operator and the so called NICA (Nonlinear Independent Component Analysis) operator, and show how a simulation bundle can be transformed into a new basis obtained from these operators. We treat aspects of the spectral approximation properties in section 4. The data analysis approach is given in section 5 and we apply the approach using the Laplace-Beltrami operator to an industrial engineering application in section 6.

2 Related Work

There are several related research works for the analysis of data from engineering simulations. A common approach for the evaluation of several simulations is the so-called sensitivity analysis. In its simplest form, one input variable is varied at a time, scalar output quantities of interest are evaluated for a few simulation results and sensitivity is measured by linear regression. Extensions of the approach in several ways are available, in particular in the form of response surface approaches [MMAC09], where the most relevant quantities of interest are trained, as fitted functions of the input parameters, based on the results of a few numerical simulations. The underlying assumption is that the information content of all simulations can be concentrated in the scalar quantities of interest. This is also the major drawback of this approach, i.e. in case the relation between input parameters and the overall behavior of the simulation cannot be reduced to such scalar quantities or is not well understood, e.g. due to complicated non-linear behavior.

In contrast to sensitivity analysis we aim to look at the data in more detail and work with the actual numerical simulation data, here only limited research did happen so far. One of the first works analyzing engineering data from full numerical simulations was Ackermann et al. [AGHH08], where the authors used principal component analysis (PCA) for detecting important parameters from nonlinear finite element simulations. Car crash simulations were analyzed in [MT08] using clustering with a local distance measure, regions of similar deformation behavior were identified and evaluated with this approach. The PCA has also been used in [TNNC10] for a group of simulations where some parameters have been changed, the approach uses the first eigenvectors of the covariance matrix of all given simulations as deformation modes. Methods based on the PCA are known to be efficient for many cases if the data variability is well reflected by the available data. The eigenvector basis from the PCA reflects those changes in an optimal way and is used to show individual deformation modes and those are even used for extrapolating new virtual simulations to show trends without calculating new time consuming simulations.

While linear methods based on the singular value decomposition (SVD), like the PCA, have proven to be successful for industrial applications, it is nevertheless known that if nonlinear correlations are present in the data, the use of the PCA is not optimal, see e.g. [LV07]. In [BGIT⁺13] several methods from machine learning have been used for the analysis of crash simulations. A preprocessing using either k -means or spectral clustering reduced the original big sized problem to several clusters, which can be analyzed separately using local linear approximation based on tangent space estimation [ZQZ11], principal manifold learning with sparse grids [FG09], and diffusion maps [CL06]. In that work, good reconstruction capabilities using the nonlinear principal manifold approach was shown as well as the detection of principal effects and the ability to detect their dependencies on certain input variables by diffusion maps. Additionally, [Iza14] shows the application of diffusion maps to the analysis of engineering data in crash simulation, vibration analysis and metal forming. The approach was able to cluster deformation data and vibration curves from simulation bundles. Furthermore, it was also shown that the most important input variable changes can be expressed using clusters in low dimensional embeddings.

Taking these research works into account, one can observe that even if good progress has been achieved, there is still need to develop methods that improve the analysis capabilities especially

in the presence of nonlinear relationships in the simulation data.

Additionally, we mention the related areas of statistical shape analysis and 3D geometry analysis. From the theoretical point, work has been done in the area of statistical shape analysis, where statistics on shape manifolds, e.g. intrinsic and extrinsic means, are studied. Started by the work of Kendall [KBCL99], this is a very active research area, recent work can be found in [SJML05, FJ07, HHM10] and references therein. A fundamental difference to methods applied in manifold learning is that in shape analysis a manifold structure of the shape space is supposed to be known and is kept fixed. Additionally, we would like to mention the mathematical work in the area of Riemannian geometries for plane curves and surfaces [MM06, BHM11], those papers, and several others referenced therein, highlight the way to the definition of an abstract mathematical setting for those spaces that can be extended to the analysis of the space of simulations.

Finally another related field is 3D geometry analysis, where the study object is a surface mesh embedded in \mathbb{R}^3 . A number of methods have been developed for pose independent shape classification [LSS⁺10], other applications include shape retrieval [RWP06], shape segmentation [RBG⁺09], invariant mesh representation [LSLCO05], and compression [BCG05], to name a few. Many of these applications make use of the Laplace-Beltrami operator specially for pose independent processing, that is, if two shapes are isometric, i.e. geodesic distances are preserved, then ideally a method will not distinguish between them. Actually this is exactly the opposite of what we want, since when we think about a deformed shape as a 3D geometry, we would like to distinguish between two isometric shapes since they are the result of a simulation with different input parameters. We also mention [OBCS⁺12], where 3D shapes are compared based on the assumption of existence of an a-priori known transformation bringing one shape into another. While this last approach has a connection to our approach, it is substantially different since it describes a shape using features which are then used for classification or pose independent shape matching. As will be seen, our approach can be interpreted expressing the same shape in another coordinate system. The intention of our approach is not to improve 3D shape analysis methods, but to be able to classify, reconstruct, estimate parameter input dependence and explore simulation data with the final objective of improving engineers productivity during the design of new products.

3 Mathematical Setting

First, we give in this section a review of the mathematical setting, in particular Riemannian manifolds, which in our case reduces to being quotient spaces of manifolds by isometric group actions. Then we consider an important component of our approach, the use of so called invariant differential operators, which have a special behavior under isometric transformations, and discrete approximations of such operators.

3.1 Preliminary Definitions

Let us start with some definitions from differential geometry, for details refer to, e.g., [Mic08]. Let φ be a distance preserving diffeomorphism $\varphi : \mathcal{M} \rightarrow \mathcal{M}'$ between two Riemannian manifolds (\mathcal{M}, g) and (\mathcal{M}', g') with $g = \varphi^* g'$, where the pullback of g' by φ is defined by $\varphi^* g' = g' \circ \varphi$. If φ is geodesic distance preserving, it follows that $d_{g'}(\varphi(p), \varphi(q)) = d_g(p, q)$, where d_g is induced by the metric tensor g . A global isometry is a map from \mathcal{M} to itself which preserves the distance function d_g .

Given a Riemannian manifold (\mathcal{M}, g) and a function $f \in C^\infty(\mathcal{M})$, $f : \mathcal{M} \rightarrow \mathbb{R}$, the differential map $d_p f : T_p \mathcal{M} \rightarrow \mathbb{R}$ is linear for all $p \in \mathcal{M}$. There exists a vector field in the tangential bundle

$T\mathcal{M}$ called the gradient of f , $\nabla_g f$ such that,

$$\langle \nabla_g f(p), X_p \rangle_{g(p)} = d_p f(X_p) \quad \forall X_p \in T_p \mathcal{M}.$$

Consider now the space $\mathcal{X}(\mathcal{M})$ of vector fields over \mathcal{M} , i.e. $X \in \mathcal{X}(\mathcal{M}), X : \mathcal{M} \rightarrow T\mathcal{M}$. Furthermore, a differential form w of grad k on \mathcal{M} is an alternating k -linear mapping $w : (\mathcal{X}(\mathcal{M}))^k \rightarrow C^\infty$, and let $\Omega^k(\mathcal{M})$ be the set of all differential k -forms on the manifold \mathcal{M} .

The interior product is the contraction of a differential form with a vector field, i.e. the map i_X is defined for $X \in \mathcal{X}(\mathcal{M})$ as $(i_X w)(X_1, \dots, X_{k-1}) := w(X, X_1, \dots, X_{k-1})$. Given a k -form $w \in \Omega^k(\mathcal{M})$, where now $k = \dim(\mathcal{M})$, and a vector field X on \mathcal{M} , the divergence $div_w X$ is defined implicitly by $d(i_X w) = div_w X \cdot w$, where $d(i_X w)$ is the exterior derivative of $i_X w$. Furthermore, the Laplace-Beltrami operator $\Delta_g : C^\infty \rightarrow C^\infty$ on a manifold is defined as $\Delta_g = -div_g \cdot \nabla_g$.

Finally, let Λ be a group of isometries of a metric space M , then Λ defines a natural group action

$$\Theta : \Lambda \times M \rightarrow M, \quad (\varphi, p) \mapsto \varphi(p).$$

The flexibility of constructing topological spaces can be enhanced through the use of equivalence relations, i.e a relation on $M \times M$ that satisfies transitivity, reflexivity and symmetry properties. Elements of M that satisfy an equivalence relation form a quotient space.

For our purposes we consider special type of quotient spaces, namely those constructed using a group Λ acting on M . If a group Λ acts on a space M by homeomorphism, then we have the orbit equivalence relation: $p \sim q$ if and only if $p = \varphi \cdot q$ for some $\varphi \in \Lambda$. Formally

Definition 3.1. *Given a group Λ acting on M , an orbit of a point p in M is the set of elements of M to which p can be moved by the elements of Λ . The set of all orbits is called orbit space and is written as M/Λ .*

3.1.1 Solution Space of Simulations

Let us now consider our abstract setting. We want to analyze the space of time dependent solutions of a partial differential equation on a given fixed domain Ω , where the variations are obtained by changing boundary and/or initial conditions. We make the following two assumptions:

- each solution at a given time is a (Riemannian) 2-manifold \mathcal{M}^i embedded, in \mathbb{R}^3 .
- solution operators are considered to be group transformations, that are assumed to be isometries, i.e. at each time step a solution \mathcal{M}^i is isometric to an initial, or reference, manifold \mathcal{M}^r .

Simulations are numerical solutions of partial differential equations and in this work we assume they are surfaces or surface functions embedded in \mathbb{R}^3 . We propose to treat them as shapes and use the Riemannian framework that has been developed for shape spaces, see [MM06, BHM11, BBM14]. According to this framework, shape space is a quotient space of a manifold modulo a group action Λ over it. For simulations we would then use, under the assumptions above, the space of orbits

$$Emb(\mathcal{M}, \mathbb{R}^3)/G(\mathcal{M}).$$

G is the group of transformations that leave a surface invariant with respect to distances as measured in the reference surface \mathcal{M}^r . Which particular structure the simulation space has will

depend on the type of group action G , e.g. one could consider rotations, translations, or deformations. A particular case, the space $Emb(\mathcal{M}, \mathbb{R}^3)/Diff(\mathcal{M})$ has been studied intensively in the more general context of embeddings in \mathbb{R}^n modulo the action of the group of diffeomorphism $Diff(\mathcal{M})$, they are shown to be special manifolds [MM06, BHM11, BBM14]. In these references also the more general case of immersions in \mathbb{R}^n is treated, those spaces are then of orbifold type due to the presence of singularities. For more details about the setting for simulations see [Ter16].

3.1.2 Discrete Setting

We view the discretization of a solution of a PDE now as a mesh approximation K of a 2-manifold \mathcal{M} , which is isometrically embedded in \mathbb{R}^3 . The following definition is one way to quantify how well a mesh K approximates a manifold \mathcal{M} , see [BSW08] for details.

Definition 3.2. *Let K be a meshed surface approximating \mathcal{M} , where the vertices of K are on \mathcal{M} . We say that K is an (ϵ, η) -approximation of \mathcal{M} if the following two conditions are fulfilled:*

- *For a face t in K , the maximum distance between any two points on t is at most $\epsilon\rho$, where ρ is the reach, defined as the infimum of the local distance between any point w in \mathcal{M} and the medial axis of the surface \mathcal{M} .*
- *For a face t in K and a vertex $p \in t$, the angle between n_t , the unit outward normal of the plane passing through t , and n_p , the unit outward normal of \mathcal{M} at p , is at most η .*

Furthermore, we have restrictions of continuous functions on \mathcal{M} to the mesh K :

Definition 3.3. *Let $f : \mathcal{M} \rightarrow \mathbb{R}$ be a continuous function on \mathcal{M} . The function f evaluated at the nodes of a mesh K is called a mesh function $f : K \rightarrow \mathbb{R}$.*

3.2 Laplace-Beltrami Operator

For the Laplace-Beltrami operator $\Delta_{\mathcal{M}} := \Delta_g|_{\mathcal{M}}$ we consider the eigenvalue problem $\Delta_{\mathcal{M}}\psi = -\lambda\psi$, restricted to the manifold (\mathcal{M}, g) , where λ is an eigenvalue of $\Delta_{\mathcal{M}}$ and ψ is the corresponding eigenfunction. We consider positive semidefinite operators, therefore all eigenvalues λ_j , $j \geq 0$ are real, positive, and isolated with finite multiplicity. The set of eigenfunctions $\{\psi_j\}_{j=1}^{\infty}$ of the operator forms an orthogonal basis for functions on \mathcal{M} , therefore the following decomposition can be written for $f \in C^{\infty}(\mathcal{M})$:

$$f = \sum_{j=0}^{\infty} \alpha_j \psi_j, \quad \alpha_j = \langle f, \psi_j \rangle_g. \quad (1)$$

For any function f as defined in (1) one can, instead of considering the function itself, equivalently consider its vector of spectral coefficients $\alpha = [\alpha_1, \alpha_2, \dots]$, obtained by projecting the function along the infinite dimensional eigenspace spanned by the eigenfunctions. Those coefficients can be used to compute the distance of functions due to the Parseval identity as follows:

Proposition 3.1. *The difference between two functions $f^1 = \sum_{j=0}^{\infty} \alpha_j^1 \psi_j$, $\alpha_j^1 = \langle f^1, \psi_j \rangle$ and $f^2 = \sum_{j=0}^{\infty} \alpha_j^2 \psi_j$, $\alpha_j^2 = \langle f^2, \psi_j \rangle$ using a decomposition with the corresponding eigenfunctions for an operator $\Delta_g(\mathcal{M})$, is given by*

$$\|f^1 - f^2\|^2 = \sum_{j=0}^{\infty} \langle \alpha_j^1 - \alpha_j^2, \psi_j \rangle^2 = \|\alpha^1 - \alpha^2\|^2$$

where α^1 and α^2 are the spectral coefficients of the orthogonal decomposition for f^1 and f^2 , respectively.

3.2.1 The Laplace-Beltrami Operator on a Mesh

Let \mathcal{M} be as before a 2-manifold \mathcal{M} isometrically embedded in \mathbb{R}^3 . Let K be an (ϵ, η) -approximation of \mathcal{M} . Further, let t be a face in K , let $\#t$ denote the number of vertices on t , and let $V(t)$ be the set of vertices of t . Then, for any vertex $w \in V(t)$ of any face $t \in K$, the mesh Laplace operator is defined as

$$L_K^h f(w) = \frac{1}{4\pi h^2} \sum_{t \in K} \frac{\text{Area}(t)}{\#t} \sum_{p \in V(t)} e^{-\frac{d(p,w)^2}{4h}} (f(p) - f(w)), \quad (2)$$

where $d(p, w)$ denotes the graph distance and h is a parameter which corresponds to the size of the local neighborhood at a point.

In the following theorem from [BSW08] one exploits that locally the Euclidean distance is a good approximation of the geodesic distance to give approximation properties for the Laplace-Beltrami operator on a surface mesh K by the mesh Laplace operator L_K^h . Notice that in [BSW08] the Euclidean distance $\|p - w\|$ is used in the definition of L_K^h instead of $d(p, w)$. Since the graph distance is a better approximation of the geodesic distance it naturally holds for definition (2) as well.

Theorem 3.2. (Laplace-Beltrami Approximation Theorem [BSW08]) *Let $K_{\epsilon, \eta}$ be a an (ϵ, η) -approximation of \mathcal{M} . Put $h(\epsilon, \eta) = \epsilon^{\frac{1}{2.5+\alpha}} + \eta^{\frac{1}{1+\alpha}}$ for an arbitrary positive number $\alpha > 0$. Then for any function $f \in C^3(\mathcal{M})$ it holds*

$$\lim_{\epsilon, \eta \rightarrow 0} \sup_{K_{\epsilon, \eta}} \left\| L_{K_{\epsilon, \eta}}^{h(\epsilon, \eta)} f - \Delta_{\mathcal{M}} f|_{K_{\epsilon, \eta}} \right\|_{\infty} = 0,$$

where the supremum is taken over all (ϵ, η) -approximations of \mathcal{M} .

According to this result, for a mesh fine enough which also approximates the curvature of \mathcal{M} well, we expect to get an approximation of the corresponding continuous Laplace-Beltrami operator on this surface.

3.2.2 The Laplace-Beltrami Operator under Isometric Transformations

We now assume that simulations are mesh functions defined on a surface mesh and that in the continuous limit a Riemannian manifold \mathcal{M}^r can be defined. Further let φ^i be a distance preserving diffeomorphism $\varphi^i : \mathcal{M}^r \rightarrow \mathcal{M}^i$ between two Riemannian manifolds (\mathcal{M}^r, g) and (\mathcal{M}^i, g^i) and let $\bar{K} = \{K^i\}_{i=1}^m$ be a set of meshes which are assumed to have the same connectivity. It is also assumed that a mesh function corresponding to $f^i : \mathcal{M}^i \rightarrow R$ is evaluated at the nodes of the mesh K^i . Furthermore, each f^i has been obtained through the transformation φ^i of one mesh function $f : \mathcal{M}^r \rightarrow R$, where \mathcal{M}^r is approximated by the mesh K^r , i.e. $f^i = f \cdot (\varphi^i)^{-1}$. The transformation is such that geodesic distances are kept the same, therefore the following diagram commutes:

$$\begin{array}{ccc} \mathcal{M}^r & \xleftrightarrow{\quad} & \mathcal{M}^i \\ \downarrow & \varphi^i & \downarrow \\ K^r & \xleftrightarrow{\varphi^i|_K} & K^i \end{array}$$

Here $\varphi_{|K}^i$ is a discrete version of φ^i . Under the above assumptions we can assert the following:

Proposition 3.3. *The approximation of the Laplace-Beltrami operator L_K^h given in (2), constructed using graph distances for one mesh $K^{i=r}$, is (approximately) the same for all meshes $i = 1, \dots, m$ in the set \bar{K} .*

Proof. Let φ^i be a diffeomorphism $\varphi^i : \mathcal{M}^r \rightarrow \mathcal{M}^i$ between two Riemannian manifolds (\mathcal{M}^r, g) and (\mathcal{M}^i, g^i) , where $g = \varphi^{i*} g^i$. Further, let φ^i be geodesic distance preserving, i.e. $d_{g^i}(\varphi^i(p), \varphi^i(q)) = d_g(p, q)$. Notice that the Laplace-Beltrami operator is invariant to geodesic preserving transformations. For any \mathcal{M}^i that is a deformed surface which is obtained from \mathcal{M}^r using a geodesic distance preserving mapping φ^i , we can therefore follow that the operator cannot distinguish \mathcal{M}^r and \mathcal{M}^i as different manifolds; we just have different charts. As a consequence, the Laplace-Beltrami operator will be the same for all \mathcal{M}^i .

Now consider a set of meshes $\bar{K} = \{K^i\}_{i=1}^m$, each K^i approximating a manifold \mathcal{M}^i , and corresponding mesh functions f^i evaluated on each K^i . We assume that through a specific transformation $f^i = f \cdot (\varphi_{|K}^i)^{-1}$, i.e. graph distance preserving, all mesh functions f^i on K^i can be obtained. Further, K^i approximates a manifold surface \mathcal{M}^i and we assume that the graph distances in K^i approximate the geodesic distances in \mathcal{M}^i . It follows that the operator (2) is approximately the same for all meshes. \square

Based on the above results, the operator can be evaluated numerically, the eigenvectors can be computed and the simulation bundle can be projected into this new eigenbasis. We make use of the expression (2), evaluated on a reference mesh. The graph distance, as an approximation of the geodesic distance, is calculated using the algorithm described in [MMP87]. To approximate the Laplace-Beltrami operator (2) we use a slightly modified version of the software¹ used in [BSW08]. That algorithm requires a parameter $\rho \cdot \sqrt{h}$ which controls the maximum geodesic distance of nodes which are employed in the calculation of a matrix entry. The overall approximation procedure is described in algorithm 1.

3.3 The NICA Operator on a Mesh Cloud

The use of the Laplace-Beltrami operator is already very useful for applications, nevertheless one can certainly think about other types of invariant operators. We introduce in this section the so-called Nonlinear Independent Component Analysis (NICA) operator [SC08], which is valid in a stochastic setting, i.e. where simulation datasets are assumed to have been obtained by sampling from an unknown probability distribution concentrated along a manifold.

Abstractly, given N points $p^{(1)}, \dots, p^{(N)} \in \mathbb{R}^d$ in the unobservable manifold \mathcal{M}^p , they are mapped to the points $\eta^{(1)}, \dots, \eta^{(N)} \in \mathbb{R}^M$ in another manifold \mathcal{M}^η by a nonlinear transformation φ . This mapping and its inverse can be linearly approximated on a ball $B_\delta(p^{(k)})$ around any given point $p^{(k)}$ by its differential. The first order Taylor expansion is then

$$\eta = \varphi(p) = \eta^{(k)} + J_\varphi(p^{(k)})(p - p^{(k)}) + O(\|p - p^{(k)}\|^2), \quad \text{for } p \in B_\delta(p^{(k)}), \quad (3)$$

where $J_\varphi(p^{(k)})$ is the Jacobian of φ evaluated at $p^{(k)}$ and also $\eta^{(k)} = \varphi(p^{(k)})$.

This expression allows a first order approximation of the distance

$$\|\eta - \eta^{(k)}\|^2 = \|J_\varphi(p^{(k)})(p - p^{(k)})\|^2 + O(\|p - p^{(k)}\|^3),$$

while for the inverse map φ^{-1} one can write

$$\|p - p^{(k)}\|^2 = \|J_{\varphi^{-1}}(\eta^{(k)})(\eta - \eta^{(k)})\|^2 + O(\|p - p^{(k)}\|^3),$$

¹J. Sun, MeshLP: Approximating Laplace-Beltrami Operator from Meshes, geomtop.org/software/meshlp

Algorithm 1: Spectral decomposition of Laplace-Beltrami operator

Input: reference simulation x^r : A surface embedded in \mathbb{R}^3 , given as triangular mesh with N points and N_f faces.

Parameter: ρ, h, p

Output: p first eigenvectors of the Laplace-Beltrami operator, invariant to distance preserving transformations

```

1 foreach  $\tilde{k} \in \{1, \dots, N_f\}$  do                                ▷ estimate areas of each face
2   foreach  $i \in \{1, 2, 3\}$  do                                  ▷ 1/3 of area assigned to each vertex
3   |  $area[\tilde{k}_i] = (\text{area of face } \tilde{k})/3$                     ▷ face  $\tilde{k}$  vertices indexed by  $\tilde{k}_i$ 
4 foreach  $k \in \{1, \dots, N\}$  do                                ▷ weight matrix with graph distances
5   |  $[ids, dists] = \text{geodist}(k, x^r, \rho \cdot \sqrt{h})$         ▷ distances on  $x^r$  up to  $\rho \cdot \sqrt{h}$ 
6   foreach  $l, d \in [ids, dists]$  do
7   |  $\mathbf{W}[k, l] = area[k] \cdot area[l] \cdot \exp(-d^2/(4h))/(4\pi h^2)$ 
8 foreach  $k \in \{1, \dots, N\}$  do
9   |  $\mathbf{D}[k, k] = \sum_{l=1}^N \mathbf{W}[k, l]$ 
10  $\mathbf{L} = \mathbf{W} - \mathbf{D}$                                           ▷ compute graph Laplacian
11 decompose  $\mathbf{L}$  by  $[\mathbf{U}, \mathbf{S}, \mathbf{V}] = \text{SVD}(\mathbf{L})$           ▷ non-trivial eigenvectors
12 return first  $p$  non-trivial eigenvectors  $\mathbf{U}$ 

```

see [SC08, KHC12] for details. In view of this approximation, a ball $B_\delta(p^{(k)})$ in \mathcal{M}^p centered at $p^{(k)}$ is therefore mapped to a small ellipsoid in \mathcal{M}^η centered around $\eta^{(k)}$. This ellipsoid can be identified with the covariance matrix $C_{k,\delta}$ of its inner points [SC08], i.e.

$$C_{k,\delta} = \mathbb{E}[(\eta - \eta^{(k)})(\eta - \eta^{(k)})^T], \quad (4)$$

by making use of the linearity of the expectation and using the approximation (3). It has been further proven in [SC08] that

$$J_\varphi(p^{(k)})J_\varphi^T(p^{(k)}) = \frac{d+2}{\delta^2}C_{k,\delta} + O(\delta),$$

where $\mathcal{M}^p \subset \mathbb{R}^d$, and that a second-order approximation of the local distance $\|p - p^{(k)}\|^2$ can be written using $C_{k,\delta}^+$, the pseudo-inverse of $C_{k,\delta}$, as

$$\|p^{(l)} - p^{(k)}\|^2 = \frac{1}{2} \frac{\delta^2}{d+2} (\eta^{(l)} - \eta^{(k)})^T \left[C_{k,\delta}^+ + C_{l,\delta}^+ \right] (\eta^{(l)} - \eta^{(k)}) + O(\|p^{(l)} - p^{(k)}\|^4)$$

Using this expression, the distance can be approximated according to the following proposition, see [SC08, KHC12] for details.

Proposition 3.4. *Let $p, w \in \mathcal{M}^p$, and let η, β be their respective mappings to the observable space \mathcal{M}^η . Then the distance in \mathcal{M}^p (using local coordinates) can be written as:*

$$\|p - w\|_{R^d}^2 = \frac{1}{2} (\eta - \beta)^T \left[(J_\varphi J_\varphi^T)^{-1}(\eta) + (J_\varphi J_\varphi^T)^{-1}(\beta) \right] (\eta - \beta) + O(\|\eta - \beta\|_{R^M}^4), \quad (5)$$

where $d \leq M$, and J_φ is the Jacobian of the transformation.

Using the distance in (5), the matrix operator of size $N \times N$ can be constructed using the weights $W_{p,w} = \exp(-\|p - w\|^2/\epsilon)$ and with it one can build the corresponding (negatively defined) graph Laplacian, for which we keep the same sign as given in [SC08],

$$L = D^{-1}W - I, \quad D_{kk} = \sum_{l=1}^N W_{kl}. \quad (6)$$

The NICA operator is now defined as L .

It has been demonstrated in [CL06] that the discrete operator L converges to a Fokker-Planck operator in the non-observable space \mathcal{M}^p , the eigenvectors of the graph Laplacian approximate also the eigenfunctions in the non-observable space in the limit $N \rightarrow \infty$, $\epsilon \rightarrow 0$

$$L_{\mathcal{M}}f = \Delta f - \nabla U \cdot \nabla f, \quad U = -2 \log \mu, \quad (7)$$

where μ is the density function in \mathcal{M}^p . As can be seen from this result, through this construction we are actually recovering an operator in \mathcal{M}^p . Additionally, it has been demonstrated that, under some conditions, the top eigenvector corresponding to the top nontrivial eigenvalue of the operator $D^{-1}W$ is actually a function of only the first non-observable variable, the second of the second one and so on, see [Sin06] for details.

We make the observation that this construction not only allows us to obtain the non-observable variables, but it delivers also an operator which is invariant to a nonlinear transformation. This constitutes a very important and interesting result for our invariant operator approach.

We propose to use this stochastic setting for the case of simulations as solutions of a PDE model subject to small parameter changes. Given m simulations, they can be assumed to be obtained as an stochastic simulation undergoing a nonlinear transformation from a reference simulation. The transformation is unknown but the realizations for different parameter combinations are known. The data points $p^{(k)}$ are assumed to have been obtained by sampling from an unknown nonuniform probability distribution μ on the manifold \mathcal{M}^p . To construct the NICA operator we take the values of the nodes of a surface mesh K , which is defined as before as an approximation of a 2-manifold \mathcal{M}^p isometrically embedded in \mathbb{R}^3 . A discrete operator for such points can be constructed as an alternative to the approximation of the Laplace-Beltrami operator considered previously.

The NICA operator is valid for one simulation, but for our setting we are considering a simulation bundle where each simulation is assumed to be obtained through a stochastic realization φ^i of a nonlinear transformation φ from a reference simulation, $\varphi^i : \mathcal{M}^r \rightarrow \mathcal{M}^i$. In this setting, available to us is a set of m simulations and our objective is to construct, based only on this information, an operator that is invariant to the nonlinear transformation φ . As explained above, such operator can be constructed. One starts with one reference simulation and takes all others to form a cloud around each point in the reference one. Then from this cloud, the covariance matrix $C_{k,\delta}$ is used to approximate the term $J_\varphi(p^{(k)})J_\varphi^T(p^{(k)})$ and its inverse to being able to evaluate (5) locally at each point k of the reference simulation. In this way the discrete operator obtained through (6) is approximately the same for each and everyone of the given m simulation data sets in the bundle. As a consequence we can write the following proposition, analogous to the proposition 3.3,

Proposition 3.5. *The approximation of the Fokker-Planck operator by L given in (6) with $W_{k,l} = \exp(-\|p^{(k)} - p^{(l)}\|^2/\epsilon)$, constructed using the distance (5) which is evaluated using the points of one reference simulation, is (approximately) the same for all simulations $i = 1, \dots, m$ in a simulation bundle, assuming they constitute a simulation cloud around the reference simulation.*

Based on the above results, the operator can be evaluated numerically, the eigenvectors can be evaluated and the simulation bundle can be projected into this new eigenbasis. We make use of the distance given in equation (5), evaluated on the nodes of a reference mesh and obtain the overall process described in algorithm 2.

Algorithm 2: Spectral decomposition of NICA operator

Input: 1) reference simulation x^r : A surface embedded in \mathbb{R}^3 , given as N points.
 2) data set bundle $\{x^j\}, j = 1, \dots, m$: Surfaces embedded in \mathbb{R}^3 , where each one is given by N points. The points of the x^j are assumed to form for each point in x^r a simulation cloud obtained by a nonlinear transformation of the reference simulation.

Parameter: δ, ϵ, p

Output: p first eigenvectors of NICA-operator, invariant to a nonlinear transformation

```

1 foreach  $k \in \{1, \dots, N\}$  do                                ▷ local Jacobi matrices at  $p^{(k)}$ 
2   empirically estimate local covariance matrix  $C_{k,\delta}$  from data set bundle  $\{x^j\}$  after (4)
3    $\mathbf{JJt}[k] = \text{pseudoinverse of } C_{k,\delta} \cdot 5/\delta^2$ 
4 foreach  $l \in \{1, \dots, N\}$  do
5   foreach  $k \in \{1, \dots, N\}$  do                                ▷ calculate weight matrix
6     estimate  $d(k, l) = \|x_k^r - x_l^r\|_{\mathbb{R}^3}$  after (5) and using  $\mathbf{JJt}[k], \mathbf{JJt}[l]$ 
7      $\mathbf{W}[k, l] = \exp(-d(k, l)/\epsilon)$ 
8 foreach  $k \in \{1, \dots, N\}$  do
9    $\mathbf{D}[k, k] = \sum_{l=1}^N \mathbf{W}[k, l]$ 
10  $\mathbf{L} = \mathbf{D}^{-1}\mathbf{W} - \mathbf{I}$                                        ▷ compute graph Laplacian
11 decompose  $\mathbf{L}$  by  $[\mathbf{U}, \mathbf{S}, \mathbf{V}] = \text{SVD}(\mathbf{L})$                 ▷ non-trivial eigenvectors
12 return  $p$  first non-trivial eigenvectors  $\mathbf{U}$ 

```

3.3.1 Illustrative example

We would like to illustrate the idea of this construction with an illustrative example from [SC08]. Let $p = [p_1, p_2]$ with p_1, p_2 uniformly distributed random variables. We are not able to observe them directly but only after a nonlinear transformations given by $\eta = [\eta_1, \eta_2]$ with $\eta_1 = p_1 + (p_2)^3$ and $\eta_2 = p_2 - (p_1)^3$. See figure 1a for a representation of the non-observable variables p and figure 1b for the observable η after the nonlinear transformation.

The Jacobian J_φ is not available, but $J_\varphi J_\varphi^T$ and its inverse can be estimated from the data. We use algorithm 2 to evaluate the operator. In the example before, we have $d = M = 2$ and can construct N (2×2) sample covariance matrices obtained from a set of m observable simulations in a simulation cloud around each point in \mathcal{M}^η . The approach assumes that a stochastic simulation can be performed for a small time step, each one starting from a different initial condition. The idea is to create a simulation burst (or cloud) around a starting or reference configuration. In figure 1c we give a representation of a simulation burst for the simple example, here for each point several stochastic outcomes are shown. By using this cloud, one calculates an estimate of the distance between the non-observable variables. Constructing the matrix operator and calculating the eigenvectors of it, one obtains the independent components. Notice that once the eigenvectors are calculated, they can be used as a common basis for the simulation cloud. All simulations can therefore be projected into the eigenbasis and one obtains as a result the spectral coefficients of all simulations.

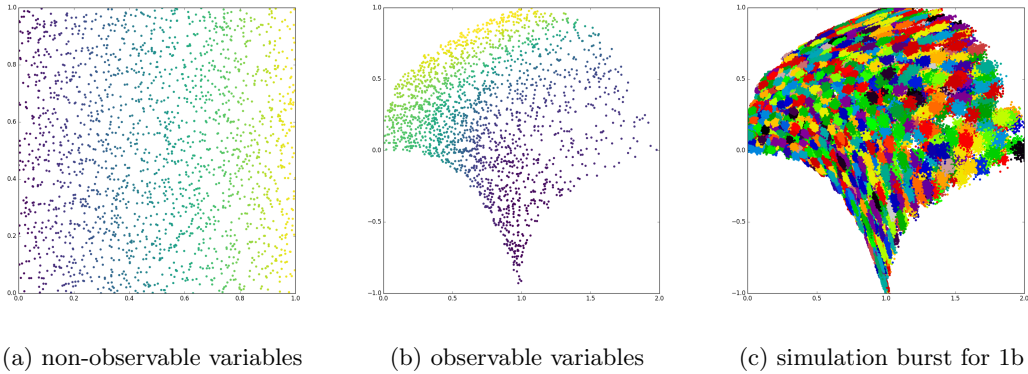


Figure 1: Illustrative example for NICA. Coloring in (a) is according to x_1 and in (b) according to the coefficient in regard to the first eigenvalue (or first independent component), which essentially recovers x_1 . In (c) the different stochastic outcomes for each point have the same color.

4 Approximating a Basis in Simulation Space

The results from propositions 3.3 and 3.5 are remarkable since they suggest that an operator can be built that is invariant to diffeomorphisms that are isometries with respect to a specific metric. In other words such an operator is the same for all elements of the space $Emb(\mathcal{M}, \mathbb{R}^3)/G(\mathcal{M})$, i.e the space of embeddings in \mathbb{R}^3 that stem from isometric transformations of \mathcal{M} . Now an orthogonal basis can be obtained from the corresponding invariant operators and it can actually be used as a basis for the space $Emb(\mathcal{M}, \mathbb{R}^3)/G(\mathcal{M})$, this means that through this construction one can characterize this space along the eigenbasis.

In the discrete setting this is achieved using the orthogonal basis of the operator given in (2) or (6), the Laplace-Beltrami operator or the NICA operator, respectively. An orthogonal basis can be constructed since both operators are valid for all elements of the corresponding simulation space, one can also project these simulations into the obtained basis in each case. Doing that, in general, will not be of any advantage since, for the case of a discrete approximation of the operators, we need as many basis elements as the number of nodes N in the mesh in order to represent each simulation. Nevertheless we will see in section 4.2 that depending on the degree of smoothness of the functions defined on \mathcal{M} , only very few basis elements are needed to recover the most important parts of the function, i.e. for smooth functions the approximation converges exponentially. We notice though, that since we are dealing with discrete data, we will have to calculate approximations of the operators and this implies that one has to actually justify the use of the eigenvectors as approximations of the corresponding eigenfunctions. This will be studied in the following.

4.1 Spectral Approximation of the Operators

We have seen in sections 3.2 and 3.3 that, under some specific conditions, a discrete operator obtained from a discrete dataset converges point-wise to a continuous operator. Nevertheless, a convergence of the eigenspace is not guaranteed in case of such an operator convergence. We now would like to describe under which conditions convergence can be expected and if it is reasonable to assume that these conditions are fulfilled in the discrete case.

4.1.1 Structure of the Eigenfunctions

The eigenfunctions of the Laplace-Beltrami operator on a surface can be viewed as a generalization of the use of a Fourier basis in Euclidean space for the Laplace operator. Using such eigenfunctions as a basis, a smooth function defined on a surface can be decomposed, so that the first spectral coefficients correspond to eigenfunctions describing the low frequency part of the function and the rest corresponds to the high frequency parts of it, see [GN13, JNT01].

For the NICA operator the eigenvector corresponding to the first eigenvalue, in increasing order, recovers the first independent component, the second one to the second and so on [SC08], see section 3.3 for the setting. Additionally, in this stochastic setting the first eigenfunctions (ordered according to increasing eigenvalues) of the Fokker-Planck operator correspond to the slow variables of a stochastic dynamical system and the independent components can be shown to be solutions of the Sturm-Liouville differential equations, see again [SC08].

The solutions of those differential equations can be shown to be generators for different type of polynomials, e.g. Jacobi, Laguerre or Hermite types, see [GUKM08]. In addition, it is also known that special solutions to the Fokker-Planck equation are polynomials that can be used in an orthogonal decomposition for less smooth functions [THJ13].

In our setting, an orthogonal decomposition based on the eigenfunctions of some specific operator will be able to decompose a function into several components. If the function f is smooth, it is known from spectral approximation theory that the decay of the spectral coefficients will, depending on the degree of smoothness of the function, achieve exponential convergence for $f \in C^\infty$, see e.g. [Cos04]. If the function is not smooth and has for example some discontinuities, it is also known that the exponential convergence is lost due to the Gibbs phenomena. But at least in regions away of the discontinuity it can be recovered or improved, see e.g. [GSSV92]. The approach to control the Gibbs phenomena consists in a change of the basis for the decomposition to special polynomials. These again can be shown to be solutions of specific Fokker-Planck type differential equations, see [THJ13]. We notice that in both cases, for smooth and, after changing the basis, for non-smooth functions we do have a few spectral coefficients that are large and correspond to the first eigenfunctions, while the rest are smaller. We will return to this observation, but first let us discuss the discrete setting.

4.1.2 The Discrete Case

In section 3.2, we have reviewed some results that allowed us to obtain convergence of a discrete mesh-Laplacian to a continuous operator given some conditions on the mesh or some large sampling limit for a point cloud. Little is known about the convergence of the discrete eigenvectors and eigenvalues to the corresponding continuous eigenfunctions and eigenvalues, this is not obtained from the convergence of the operators. This area is an active field of research, we mention the following result that follows from [DRW10]:

Theorem 4.1. *Given a smooth 2-manifold \mathcal{M} and a simplicial mesh K which is an (ϵ, η) -approximation of \mathcal{M} . Let $\{\lambda_j\}$ and $\{\lambda_j^D\}$ denote the set of non-decreasing discrete eigenvalues of the Laplace-Beltrami operator $\Delta_{\mathcal{M}}$ and its approximation L_K^h (2), respectively. For any fixed j , we have that*

$$\lim_{h, \epsilon, \eta, \frac{\epsilon}{h^4} \rightarrow 0} |\lambda_j - \lambda_j^D| = 0.$$

The question of convergence of the eigenfunctions using the same construction as given in [DRW10] is to our knowledge open. We also mention the work in [RBG⁺09], where the Laplace-Beltrami eigenvalue problem is discretized using a finite element formulation and as such can be constructed using convenient convergence properties depending on the mesh size and the degree

of the shape functions used for the discretization, although the convergence to the eigenspace has not been treated in this work either. Note that in our case we would like to build an operator based on the data, so that we have not the flexibility of choosing a discretization like in [RBG⁺09].

A different setting to proof convergence is the stochastic one, based on convergence in probability. We mention here the work in [BN08] where it has been shown that the eigenstructure of the weighted graph Laplacian converges to that on the manifold and a recent result that extends such results for the so called Connection Laplacian, where the convergence to the Fokker-Planck operator is treated as special cases of the more general setting of the Connection Laplacian [StW13].

To summarize, based on the mentioned results, the use of a discrete approximation of the eigenfunctions of the Laplace-Beltrami and NICA operators can, to a certain extent, be justified for our approach.

4.1.3 Discrete Orthogonal Decomposition

Once the eigenvectors $\bar{\psi}_j$ of some specific discrete operator are given, we can project a given mesh function f^i defined on a mesh K^i along them and obtain as a result a set of spectral coefficients $\alpha_j^i, j = 1, \dots, N$. The following expression can be written as an analogous expression of the continuous case (1):

$$f^i = \sum_{j=1}^N \alpha_j^i \bar{\psi}_j, \quad \alpha_j = \langle f^i, \bar{\psi}_j \rangle, \quad (8)$$

where N corresponds to the number of nodes on the mesh K^i , which can be very large. Using the approximation L_K^h of the Laplace-Beltrami operator a large number of eigenvectors could be necessary to reconstruct the mesh data, depending on the smoothness of the data, which directly affects the degree of decay of the spectral coefficients. Nevertheless, the corresponding spectral coefficients will be large for the coarse parts of the finite element mesh and smaller for the details. Note that this is a direct consequence of the exponential decay that has been observed for the continuous case. Such a decay can intuitively also be expected in the discrete case, assuming convergence conditions for the eigenspace are valid, both for the Laplace-Beltrami operator and the NICA operator. For non-smooth functions we could instead use eigenvectors of the NICA operator, which are actually approximations of general polynomial functions and better adapted to the non-smoothness of the data as discussed in section 4.1.1.

Now assume K^r is a mesh which approximates the reference manifold \mathcal{M}^r . Let $\mathcal{M}^i, i = 1, \dots, m$ be the manifolds obtained by the application of diffeomorphisms φ^i with corresponding approximations given by $\varphi^i|_{K^i}$ on the mesh K^i . Let the function $f : \mathcal{M}^r \rightarrow \mathbb{R}$ be evaluated at the nodes of the mesh and let $f^i : \mathcal{M}^i \rightarrow \mathbb{R}$ be the resulting functions after the application of φ^i . The functions f^r, f^i correspond in our setting to the numerical solutions of a partial differential equation using the finite element method. Further, for simplicity we assume that the functions f^r, f^i are k -times differentiable. Under these conditions the following holds:

Proposition 4.2. *Let an orthogonal basis consisting of N eigenvectors $\psi_j, j = 1, \dots, N$ be given, which is obtained from the approximation of the Laplace-Beltrami operator (2). Then all mesh functions f^i can be represented as*

$$f^i = \sum_{j=1}^N \alpha_j^i \psi_j,$$

where α_j^i are the spectral coefficients obtained by the projection of f^i into the eigenvector basis $\{\psi_j\}_{j=1}^N$.

Proof. This is a consequence of the application of (2), under the assumption that the basis is invariant under isometric transformations, see proposition 3.3. \square

For the NICA operator (6), we are in a stochastic setting. Let a set of simulations be represented as functions $f^i : \mathcal{M}^r \rightarrow \mathbb{R}$ obtained as realizations of an independent stochastic Ito process. This operator approximates a Fokker-Planck operator which is invariant to a nonlinear transformation as considered in section 3.3. Furthermore, we assume convergence in probability to the eigenfunctions of the continuous NICA operator. Under these conditions, we can write

Proposition 4.3. *Let an orthogonal basis consisting of N eigenvectors ψ_j , $j = 1, \dots, N$ be given, obtained from the approximation of the Fokker-Planck operator as given in (6), then all functions f^i can be represented as*

$$f^i = \sum_{j=1}^N \alpha_j^i \psi_j, \quad (9)$$

where α_j^i are the spectral coefficients obtained by the projection of f^i into the eigenvector basis $\{\psi_j\}$.

Proof. This is a consequence of the application of equation (6), under the assumption that the basis is invariant under nonlinear transformations (see proposition 3.4). \square

As explained in the previous sections, we use operators that are invariant under a specific transformation. As a consequence we can project a set of mesh functions along the same basis for functions defined on a set of meshes. This property, combined with the observation about the possibility of achieving a strong decay behavior of the spectral coefficients, suggests a method for data analysis which potentially reduces the dimensionality of the data along the spectral coefficients. In other words, only a few coefficients correspond to large variations in the finite element data (the coarse ones) or to the slow variables in an stochastic system for more general point clouds, respectively.

4.2 Approximation Properties

Note that we here only consider the stochastic setting. We will show that under some conditions one can expect a strong decay of the spectral coefficients depending on the orthogonal functions used and the smoothness properties of the data.

As before, we focus on numerical simulations, where we know the approximation properties since the data stems from a finite element mesh which discretizes a partial differential equation. The smoothness of the solution, combined with the considerations about the spectral approximation estimation based on discrete data, allows us to obtain an estimation that depends on the smoothness of the function and therefore clarifies the observed strong decay of the spectral coefficients, at least for a simplified setting.

We assume that we have obtained an orthogonal decomposition (9), then the following result holds

Proposition 4.4. *(Decay of the Spectral Coefficients) In the orthogonal expansion given in (9), under suitable assumptions the first few coefficients decay very fast, depending on the degree of smoothness of the functions $f^r, f^i, i = 1, \dots, m$.*

For the proof we combine the following three results.

Proposition 4.5. [SC08] *Given the eigenvalue problem for the Fokker-Planck operator (7), the operator can be separated by the use of an orthogonal transformation and it can be shown that the separated problems are 1D backward Fokker-Planck-like operators with Neumann boundary conditions. The solution of the eigenvalue problems with such operators corresponds to the solution of Sturm-Liouville problems.*

Note that the density function μ in (7) is separable [SC08], therefore the solution is obtained in terms of 1D Sturm-Liouville problems with Neumann boundary conditions.

We now consider the solution of the 1D Sturm-Liouville problem. It is known, see [Moh06] and the references therein, that solutions of the 1D Sturm-Liouville eigenvalue problems for specific boundary conditions are orthogonal polynomials. Such polynomials can be used as a basis for a spectral approximation of a general function f .

Proposition 4.6. *Let $f \in C^k$ and its spectral approximation be given by $f_N = \sum_{j=1}^N \langle f, \psi_j \rangle \psi_j$, where ψ_j is an orthogonal polynomial solution of a Sturm-Liouville eigenvalue problem, then the following holds,*

$$\|f - f^N\| \leq \frac{C}{N^k}.$$

In particular if $f \in C^\infty$, then it can be shown that the decay is exponentially fast, i.e if

$$\epsilon_N = |f - f_N| = \sum_{r>N}^{\infty} \langle f, \psi_r \rangle \psi_r,$$

then for this case

$$\epsilon_N = O(e^{-cN}), \quad c > 0.$$

Continuing in view of the main result, we notice that proposition 4.6 cannot be used directly for our case since only discrete data is available there. To be able to apply the continuous result to the discrete case we need the next result

Proposition 4.7. [DJ94] *The estimation error between a function and its discrete approximation is related to the N -term approximation using an orthogonal basis function decomposition and the rate of decay depends on the smoothness of the continuous function that is approximated.*

Now we have all elements that help us to give a sketch of the proof for proposition 4.4, for full details see [Ter16].

Proof sketch. By proposition 4.5 we know that the continuous Fokker-Planck operator (7) is separable into 1D Sturm-Liouville problems whose solutions are orthogonal polynomials. From spectral theory (see proposition 4.6) it is known that the decay of the spectral decomposition of a general function f using orthogonal polynomials depends on the smoothness of the function f . Finally using proposition 4.7, we justify this last result for our case, where we only have discrete data approximating f . \square

5 Data Analysis Method

Our application interest is the analysis of many simulation results which are obtained from the numerical solution of PDEs with finite elements. In previous sections we developed a theoretical setting which enables us to develop a new method for analyzing the (quotient) space of simulations.

5.1 Method Fundamentals

Let us recapture the elements of our method:

- a transformation group Λ , for example $Isom(\mathcal{M})$
- a metric space $Emb(\mathcal{M}, \mathbb{R}^3)$, where the group acts on
- invariant generalized coordinates of $Emb(\mathcal{M}, \mathbb{R}^3)/G(\mathcal{M})$
- a transformation, which we call the invariantization transform, sending an element of $Emb(\mathcal{M}, \mathbb{R}^3)$ to the invariant space $Emb(\mathcal{M}, \mathbb{R}^3)/G(\mathcal{M})$.

As before, we assume that all simulations stem from a 2-manifold \mathcal{M} . Additionally, we use a discrete representation of a function f^i evaluated on a mesh K^i . The data analysis method now consists of the following steps, see also algorithm 3:

1. construct a positive semidefinite operator that is invariant to a specific transformation,
2. obtain an orthogonal decomposition using as basis the eigenvectors of the operator,
3. project the dataset into this orthogonal basis.

Usually one performs a thresholding of the coefficients based on the decay properties.

Algorithm 3: Algorithm for Dimensionality Reduction

Input: m simulations $f^i \in \mathbb{R}^N, i = 1, \dots, m$, where N is the number of nodes

Parameter: embedding dimension p

Output: reduced representation $[\hat{\alpha}^1, \hat{\alpha}^2, \dots, \hat{\alpha}^m]$ with each $\hat{\alpha}^i \in \mathbb{R}^p$

- 1 $\mathbf{U}_p = p$ first eigenvectors of either the Laplace-Beltrami operator (algorithm 1) or the NICA operator (algorithm 2)
 - 2 **foreach** i in $\{1, \dots, m\}$ **do**
 - 3 $\hat{\alpha}^i = \mathbf{U}_p \times f^i \in \mathbb{R}^p$ \triangleright compute p -dimensional embedding
-

In a certain sense we obtain in step 3 invariant coordinates due to the eigenvector basis, which is a discrete approximation of the basis of the space $Emb(\mathcal{M}, \mathbb{R}^3)/G(\mathcal{M})$. Since the basis is obtained from an invariant operator, these projection coefficients reflect the group action required to obtain a specific simulation. As seen in section 4.2, under some conditions the coefficients have a strong decay, therefore the “essential” part of a dataset is concentrated in a few coefficients. This allows a dimensionality reduction of a data set of simulations in a multi-scale fashion. As shown, and will be seen in the experiments, the first few coefficients correspond to the essential parts, the later ones are less relevant and can be geometrically associated with high frequency parts or details, at least for the Laplace-Beltrami operator. Depending on the decay of the coefficients, we can use only the first few spectral coordinates to analyze the variability of all simulation data.

Note that such a method for dimensionality reduction of a simulation bundle can be justified by using the invariance and the approximation results of the previous sections applied to such a bundle. Assuming enough regularity of the functions being approximated by the simulations, the obtained approach establishes that the essential principal variations of a dataset bundle correspond to the coarse variations and that the other variations concentrate along the details. We express this using the following corollary of proposition 4.4.

Corollary 5.1. *A multi-scale dimensionality reduction of a data set bundle $\{f^i\}_{i=1,\dots,m}$ can be achieved using the spectral coordinates $\alpha_j^i, i = 1, \dots, m, j = 1, \dots, N$ found by projecting all simulations to the same orthogonal base constructed with an invariant operator. The low dimensional part corresponds to the coarse variations of the data set bundle.*

Note that up to dimension three the projection coefficients can be used directly as embedding coordinates for visualization. If more coefficients are required to capture the data, a further method of dimensionality reduction can be used to obtain an embedding up to dimension three. In particular, we use diffusion maps for further dimensionality reduction [CL06, BGIT⁺13, Iza14]. This method constructs a similarity matrix between the simulations based on their projection coordinates and uses the eigenvectors of this matrix, after a normalization, to obtain low dimensional embedding coordinates.

Use of a single spectral basis for all simulations also naturally enables the construction of low dimensional representations for time dependent problems. Given a time dependent data set, one repeatedly calls algorithm 3 for each time step.

To summarize, the approach using the described eigenbasis has the following properties:

- A reconstruction of simulation data based on only a few coefficients ($p < 20$) with a small error (usually $< 5\%$).
- An extraction of useful low dimensional information in the largest spectral coefficients that parameterize all data.
- A natural simultaneous treatment of many time steps.
- A reconstruction of out-of sample data not available in the training set with good precision. In other words, simulations for a specific input parameter combination, not in the training set, can be approximated based on the given training data and embedding coordinates.

These properties of our multi-scale approach will be demonstrated in section 6 on real problems.

5.1.1 Comparison with Principal Component Analysis

Due to its simplicity, the PCA is one of the most employed methods for dimensionality reduction [LV07], we compare against it as a baseline method. Given a dataset $X = \{X^1, X^2, \dots, X^m\}$, $X^i \in \mathbb{R}^n$ a very efficient way of representing the variability of the datasets is the SVD decomposition given by $[USV] = svd(X_c)$, where X_c is a centered representation of X , U is a matrix, S is a diagonal matrix whose diagonal elements are the singular values corresponding to the eigenvectors in U , and V is the complementary base. If the eigenvalues are ordered in descending order, then the first eigenvector correspond to the first main variation of the dataset, the second to the second and so on. Often only a few coefficients are necessary to reconstruct each data so that $X^i \approx \sum_{k=1}^p \langle U_k, X^i \rangle U_k$ with $p < m \ll n$. The approach then reduces to the calculation of p eigenvectors. Underlying the PCA is also the preservation of Euclidean distances in the high dimensional space [LV07].

In the case of numerical simulations in a finite element space, each simulation can be considered as a point in $\mathbb{R}^n, n = 3N$, where N is the number of vertices, in order to apply the PCA. Comparing the basis for the PCA, Laplace-Beltrami operator and NICA operator one observes significant differences. PCA can concentrate the variability of the data in just m coefficients, where m is the number of simulations available. The other operators are bigger, of the order of the number of nodes N , but the first coefficients are large in comparison with the rest and

that is the reason why we use them for data analysis. Those coefficients can be shown to be related to the coarse part of the geometry for the Laplace-Beltrami operator [KG00] and to the first nonlinear components for the NICA operator [SC08]. For the PCA, if we attempt to view it as an operator, the first coefficients are related to the variability of the data and not to a smooth part of the geometry nor any nonlinear component. While the PCA recovers in the first 3 coefficients more information than any of the other methods, unfortunately this fact can be used only if the variability of the data can be adequately represented based on those coefficients. If the data is localized around a nonlinear manifold or, in other words, if there is some nonlinear dependence on a few intrinsic parameters, then other methods are needed. The operator approach suggested in this paper proposes a way to obtain the information about this low dimensional structures, we can decompose the data variability in a flexible way by changing the operator, which is constructed to preserve some quantity or property.

5.2 Operator Invariance Dependence

Taking a closer look at the proposed method, the important step is the construction of the operator. For example pose invariance of a deformation can be achieved using an approximation of the Laplace-Beltrami operator constructed using geodesic distances in the finite element mesh. For an stochastic Ito process one can even obtain invariance to a general nonlinear transformation. After obtaining discrete approximations of these operators, we project the data to the eigenvectors of the spectral decomposition and obtain a new representation. Assuming a decreasing order of the eigenvalues and a fast decay of the spectral coefficients, most of the “energy” of the data is concentrated in the first few components.

In the continuous case, it has been shown that the operators we use have a discrete spectrum and that additionally the eigenfunction build a multi-scale decomposition using nodal sets [RBG⁺09]. Those properties are also available under the discussed convergence conditions for the discrete case, so that the proposed analysis method has a multi-scale structure which is also flexible, in the sense that one can influence what is considered as coarse scales through the local invariant distance. For example in case of the Laplace-Beltrami operator we have the usual decomposition of a mesh function into coarse parts and details; using a NICA operator our scales will be the independent components.

The approach is very flexible if we manage to identify the correct invariant operator corresponding to the way simulations are assumed or observed to behave under change of parameters. Let us recall the invariance property for the investigated operators according to this. For example, if they show only rigid changes (rotations or translations), then we can use a Laplace-Beltrami operator with a kernel using the Euclidean distance since this operator is rotation and translation invariant. In the case of non-rigid transformations like deformations that modify the shape arbitrarily, but does not tear or shrink the shape, we can use the Laplace-Beltrami operator with a kernel using a geodesic distance approximated in the mesh by the graph distance. The operator constructed in this way will then be invariant to deformations that preserve geodesic distances. Finally, we could also have an arbitrary nonlinear transformation that brings one simulation to the next one, employing the NICA operator we obtain an invariance to such a nonlinear transform.

6 Applications for the Analysis of Finite Element Simulation Bundles

Finite element simulations in industry are nowadays used to study the physical behavior of products. We consider the example of car parts under deformations due to a crash. The development of new car models demands the creation of thousands of simulations where some material parameters or the geometry are varied. The analysis of the combined effect of those changes in the crash behavior is an open problem and designs are nowadays made based on engineering judgment in a time consuming trial and error process. We illustrate in this section the application of our proposed data analysis method to the case of crash simulations. While all three operators outlined in section 5.2 can achieve an effective dimensionality reduction for this data, we will concentrate on the Laplace-Beltrami operator with geodesic distance to focus and simplify this section. Results for the NICA-operator will be presented in a companion paper.

6.1 Finite Element Signal Decomposition

First, we investigate the decomposition into coarse parts and details of a function on a mesh stemming from crash simulations. We consider a frontal crash simulation of a Chevrolet C2500 pick-up truck, a model with around 60,000 nodes from the National Crash Analysis Center². We use 126 simulations³ of a vehicle frontal crash where 9 part thicknesses are varied randomly by up to $\pm 10\%$. The variation in the thickness of these 9 parts results in different deformations of the original structure, see also [BGIT⁺13]. The approximation of the Laplace-Beltrami operator using geodesic distances is calculated as described in section 3.2 using the initial mesh configuration. The eigenvectors of the operator can then be used to evaluate the scalar product $\alpha_j^i = \langle f^i, \psi_j \rangle$ and obtain the spectral coefficients for any mesh function.

6.1.1 Decompositions of Deformation and Mesh Associated Variables

The deformations of the mesh for one simulation are now the considered mesh functions f^i , one for each coordinate x, y and z , i.e. 3 per simulation. Using the same connectivity of the original mesh, we can reconstruct the mesh deformations, separately for the x, y , and z coordinates, using $f^i = \sum_{j=1}^p \alpha_j^i \psi_j$ for several values of p .

From figure 2a, it can be clearly seen that using $p = 20$ only a very coarse approximation of the part can be reconstructed. Adding more values, e.g. $p = 100$, recovers more details of the part. It can also be clearly seen in figure 2b that most of the coefficients are small, with a few bigger ones. This is an essential feature which will be exploited for a classification task in section 6.1.2.

So far, we were able to show that the geometry of a car part can be represented using an orthogonal basis of the eigenvectors of an operator. But, any function $f \in C^k(M)$ on the mesh can be represented by the linear combination of the eigenvectors. This implies that also other variables associated to each node can be represented using the same orthogonal basis, this can be used for variables like nodal strains, temperatures, velocities, and so on.

We now demonstrate this with an example, where the nodal variable is the absolute difference between two time steps (6 and 7) of the car crash simulation. For figure 3 the difference is reconstructed using different values of p and it can be seen that with $p = 20$, compared with $p = 200$ and with the original data, almost the original color distribution is obtained for the nodal variable.

²<http://www.ncac.gwu.edu/>

³Computed with LS-DYNA <http://www.lstc.com/products/ls-dyna>

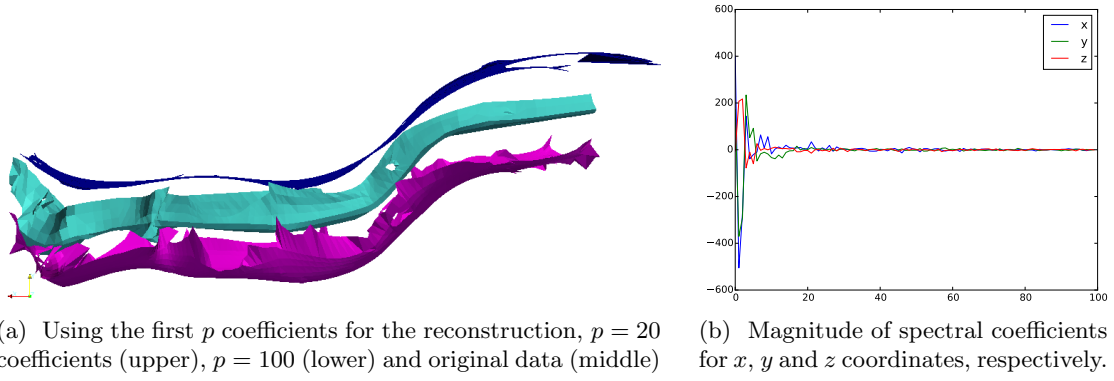


Figure 2: Analysis of a multi-scale reconstruction of a deformed shape.

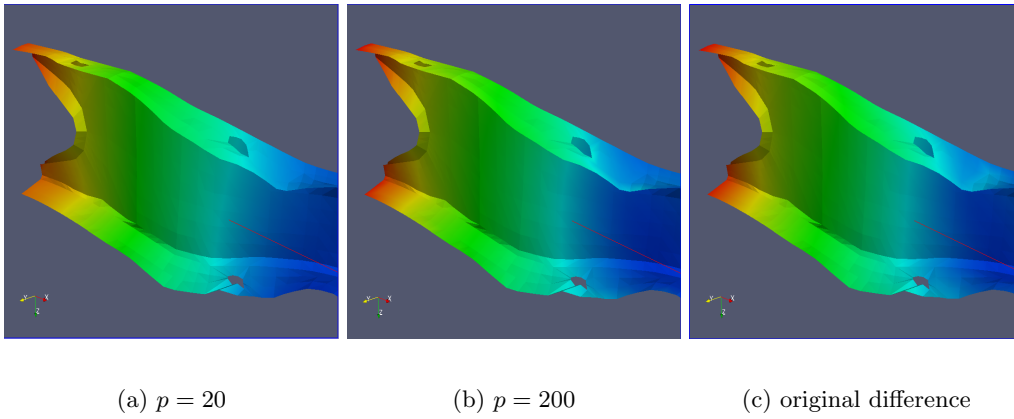


Figure 3: Reconstruction of the differences between two time steps using p coefficients.

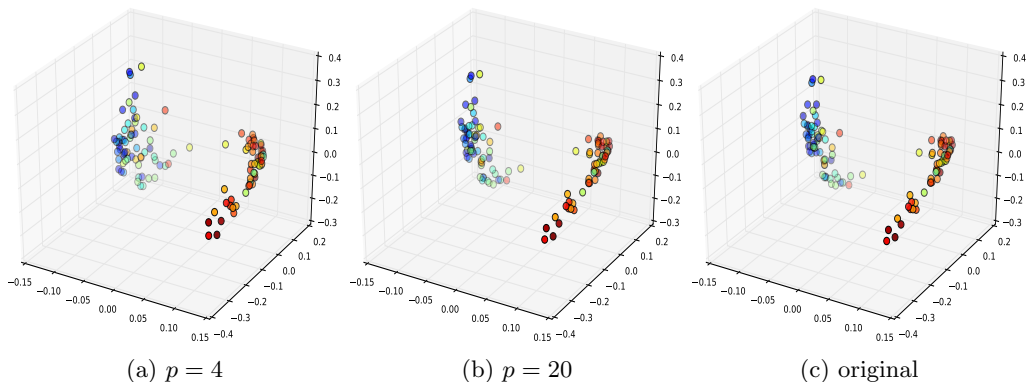


Figure 4: Comparison of diffusion maps embeddings for the car crash data using different number of spectral coefficients in the distance computation between the data points.

6.1.2 Data Analysis of Deformations in Crash Simulations

In [BGIT⁺13] this data set was used for nonlinear dimensionality reduction. There, the norm of the difference of the deformations between the two time steps 6 and 7 was used as the nodal value. A total of $m = 116$ simulations were used with $f_k^i = \sqrt{\|x_k^i - y_k^i\|}$, where $x_k^i, y_k^i \in \mathbb{R}^3, k = 1, \dots, N = 1714$, and x_k^i, y_k^i denote the position of grid point k of simulation i at the time step 6 and 7, respectively. Based on this $m \times N$ dimensional data a lower-dimensional embedding was computed using diffusion maps, see [BGIT⁺13, Iza14] for details. With this data analysis approach one was able to successfully identify buckling modes and input parameter dependences.

To demonstrate the usefulness of our approach we investigate the use of the spectral coefficients as input to the nonlinear dimensionality reduction procedure. We project as before all m vectors f^i along the eigenvectors of the approximation of the Laplace-Beltrami operator obtained in section 6.1. The result is a set of coefficients also in \mathbb{R}^N , where N is the number of nodes of the deformed beam. The coefficients decay very fast, i.e. similar to figure 2b, the energy of the signal is concentrated in very few coefficients and, as we presented in the theoretical part, one can equivalently use these coefficients instead of the original vectors of differences. Due to the decay, we just would like to keep the most significant ones and compare the embedding with diffusion maps using the first $p = 4$ and $p = 20$ coefficients with the embedding obtained using all the differences in \mathbb{R}^N . Figure 4 shows a comparison of these embeddings, where each point corresponds to the embedding of one f^i . The color of the points is given by the value of one of the varied plate thicknesses. It shows that this one has a high correlation with the resulting clustering of the deformation results and therefore graphically verifies the differences in the classification due to the eigenvectors.

It is interesting to see that with only $p = 4$ the structure of the embedding is almost the same and can be used for classification instead of using the original information of size $N = 1714$. This has a number of implications, but the important one is that the embedding is actually completely dominated by the first few components in the orthogonal decomposition, which correspond to the coarse variations.

6.2 The Pre-image Problem in Crash-Simulation

The use of dimensionality reduction in applications is characterised through the interplay between the so called restriction and extension phases. This has already been studied in several applications like image processing and earth structure classification, see [TESK11, KHC12]. We elaborate on this for a particular application in crash simulation.

Given a training set of data in a high dimensional space \mathbb{R}^N , dimensionality reduction methods extract a low dimensional representation in \mathbb{R}^p , $p \ll N$ in such a way that each of the training data can be identified with an element in this new space, this is sometimes called the restriction phase. Such a mapping can be done in several ways and generally one tries to preserve some property of the high dimensional space like geometric distance or the topology (see [LV07] for a detailed description). The structure of the embedding should allow to find the corresponding position in the lower dimensional space for any new test data point in the higher dimensional space.

Ideally, after obtaining this parameterization, one would like to obtain a high dimensional approximation that corresponds to a specific point in the low dimensional representation not in the training set. This is very important for applications in image segmentation and denoising. Given some embedding coordinates, this so called extension phase now enables the reconstruction of the corresponding high dimensional data set in \mathbb{R}^N . This is an ill posed problem since the same embedding coordinates could correspond to different high dimensional extensions. How to find them is known as the pre-image problem and has been extensively studied and is still an open problem, see e.g. [KHC12].

The use of the proposed operator approach introduces a transformation with a fundamental simplification, the pre-image now gets parameterized with very few coefficients that are able to reconstruct a coarse version of the analysis quantity, e.g. in the example from section 6.1.2 with as few as four parameters.

We now investigate the application of the method to the pre-image problem in crash simulation, where it has another very interesting property, namely it corresponds to obtaining an approximation of a numerical simulation without using the finite element software. Note that crash simulation is a highly nonlinear process and trying to interpolate between existing simulations based on the original input parameter space will in general not produce satisfactory results. Since one simulation of a real model in the car industry takes several hours using up to hundreds of computing nodes, the advantage is clear if one would be able to get an approximate behavior without investing that huge amount of computing resources. An approach in this direction was presented in [BGIT⁺13].

We use again the data set from section 6.1, a frontal crash simulation a truck with around 60,000 nodes and 17 time steps. A total of 126 simulations were obtained by varying randomly the thickness of 9 structural components, 116 data sets are used for the training phase and 10 data sets are used for testing the approach. As in section 6.1.2 the difference between time step 6 and 7 is used as our analysis variable. Figure 5 shows two examples of the distribution of the values of the difference on the analyzed part (we take the difference between two arbitrary selected datasets), as expected the squared differences are large for arbitrary selected datasets.

We use the training data set and construct an operator as described in section 6.1.2, to find a low dimensional embedding. For the 10 test data, we use only the coordinates in the 3D embedding and based only on these coordinates, we take the immediate nearest neighbor as an approximation to the actual low dimensional embedding coordinates of the test data. Note that we do this only to measure the quality of the low dimensional embedding in predicting the relative positions of the data in the low dimensional setting, and use this as an indication for the reconstruction properties. Figure 5c shows the mean of the error over 10 reconstructed data

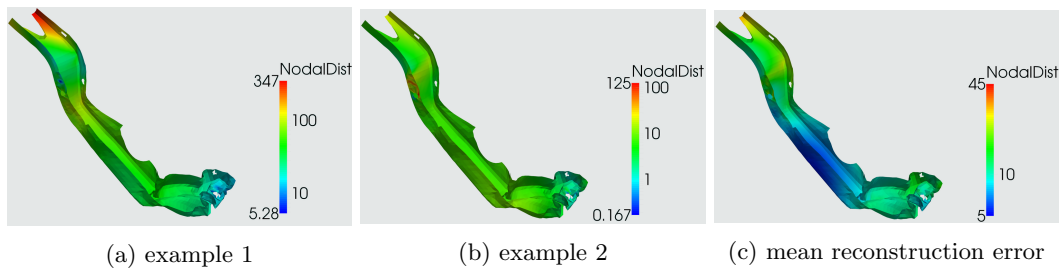


Figure 5: a), b): We consider deformations between two consecutive time steps. Shown in each picture are the differences of the deformations between two arbitrarily chosen simulations from the training data. c): Mean of the reconstruction error over 10 test data.

sets. For other nonlinear dimensionality reduction procedures, e.g. diffusion maps, we observed in the course of our research that using the nearest neighbor in the low dimensional coordinates does produce on average worse “reconstruction” results.

We can see that using the embedding coordinates from the training set a reconstruction of simulation results of several test data appears possible. The results shows that we can obtain a rather good approximation of the high dimensional test data as measured by the mean of the error for all test data sets, see figure 5c. A detailed investigation of this approach for the reconstruction or prediction of “virtual” numerical simulations using a combination of the eigenvectors is surely warranted, but out of scope of the current work which focuses on data analysis.

6.3 Time Dependent Analysis of Crash Simulations

The properties of the introduced approach allow also the efficient analysis of time dependent information, this is due to the use of a common basis for all simulations and time steps. Car crash simulations are strongly time dependent, in very few milliseconds the structure of a car can deform strongly. Furthermore, an unstable behavior can originate from small variations in the material properties, initial load conditions or numerical conditioning. This phenomenon is called buckling and is a serious problem for the robust design of car components. Relevant for an engineer is not only the identification of principal bifurcation modes, but also the study of the time of origin of the unstable behavior.

Our approach now allows a time dependent analysis of such unstable deformation characteristics. We use the same Chevrolet truck example as before, but to visualize the time dependent behavior we employ more time steps and therefore now use 167 simulations and 141 time steps, where again 9 plate thicknesses are varied. Figure 6 shows an example where the deformation behavior over time for these simulations is displayed, where the color indicates the time. To obtain the shown 3D embedding we proceed along the lines of section 5 using the Laplace-Beltrami operator in algorithm 3 for the initial mesh and using the obtained eigenvectors to represent all simulations over all time steps.

There are several observations that can be made from the obtained configuration in figure 6. We see that the reduced coordinates of the simulations give an organization of the data in time. A bifurcation clearly starts about half-way during the crash simulation, while one can see how the positions of the simulations for the last time steps appear mixed with those before. This corresponds with the rebound effect in a crash, where the car bounces back from the obstacle after the inertia of the movement was absorbed.

Other embedding methods can be applied to the same data, but dealing with all time steps

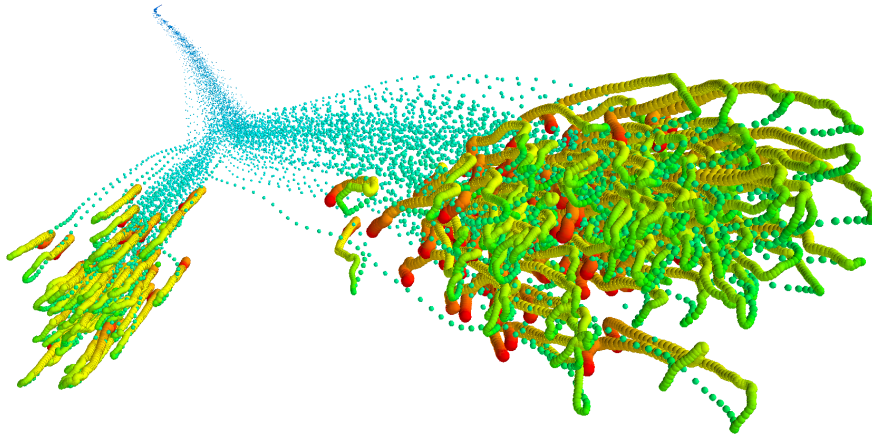


Figure 6: Reduced 3D representation of 23547 (167 simulations \times 141 time steps) time dependent simulation results, obtained by the spectral decomposition of the Laplace-Beltrami operator. The coordinates of each point, which indicates a simulation at a specific time, are the first spectral coefficients for each direction x , y , and z of the movement of the car, they are colored according to the corresponding time step of the simulation.

simultaneously is very limited. The usual approach is to use the PCA for time dependent analysis as well, so as a first example let us calculate it using all simulations from one time step, where the bifurcation is clearly present. The spectral coefficients obtained by projecting the deformations for some selected time steps along these principal components gets the low dimensional structure shown in figure 7a, this approach does not produce adequate results since the variability over all time steps is not taken into account. Computing a PCA using all simulations and time steps does improve the results, but only to some degree, see figure 7b. Although a time behavior is now visible and a small separation is recognizable near the end, the clear separation and different results due to the bifurcation cannot be recognized in the embedding, in particular not the time of origin as is the case in figure 6.

Other nonlinear dimensionality reduction methods could in principle be used for dealing with this data set. But then, either the embedding method has to be computed as many times as time steps are available, where the switching of the eigenvectors makes recovering a time dependent low dimensional structure very cumbersome, if at all possible. Alternatively, one could attempt to embed other time steps into the coordinates obtained from one time step using the Nyström method, but this is as limited as the PCA example before. Using all simulations and all time steps is not feasible since one has to deal with large full matrices, and cannot go to a formulation in the size of the mesh, or relevant parts of it, as is possible for PCA or our approach.

7 Summary and Discussion

Investigating bundles of finite element simulations in industrial applications is a challenge, due to the high dimensionality and complexity of the dataset. We presented an analysis approach that can cope with this problem based on a new method for dimensionality reduction. The method is based on the assumption that all simulations are obtained from the transformation of a reference configuration, in particular we pose this problem in an abstract setting where all simulations are

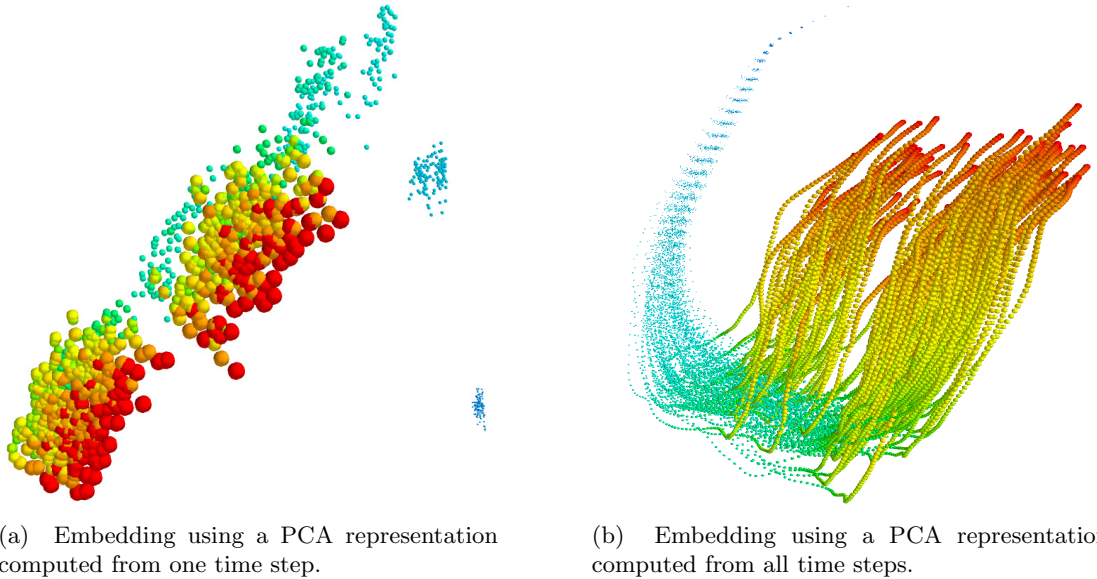


Figure 7: Reduced 3D representation of simulations over several time steps, obtained with PCA. The points indicate a simulation at a specific time and are colored according to the corresponding time step of the simulation.

in the quotient space of all embeddings of a manifold in \mathbb{R}^3 modulo a transformation group. All simulations are represented in a new basis derived from an operator invariant to a specific transformation group, it is shown that under certain approximation conditions only few components are required in this new basis to recover the essential behavior of the simulation data. Industrial examples are presented that show the properties of this new method.

The presented first applications of this method show promising possibilities for the analysis of finite element data from simulation bundles. Further research is necessary in order to analyze the consequences of the assumptions made on the theoretical setting, analyze the use of other operators invariant to a more general transformation, e.g. not in the setting of stochastic realizations, and also whether there are other areas where this analysis method can be used.

The use of a new basis that capture intrinsic properties of the dataset demands on the one side a larger number of components than using principal component analysis, on the other hand this is precisely necessary to allow for a larger range of degrees of freedom that are not available using principal component analysis. We conjecture, that the use of this larger basis in a learning setting provides a much better generalization ability for cases that are not available in the training set. Noting that considerable efforts are invested in industrial product development for finding optimal designs in a global optimization approach, which is highly compute intensive due to the large amount of variables, we conjecture that the use of the proposed method has the potential to reduce this complexity by several orders of magnitude.

From the theoretical point of view, we used an abstract setting that incorporates the general framework of shape analysis for this type of data. The link to the theoretical treatment of the quotient space $Emb(\mathcal{M}, \mathbb{R}^3)/Diff(\mathcal{M})$ is to be explored in more detail, especially if one would like to evaluate geodesics as in the shape space setting. This introduces the research question of designing efficient algorithms for calculating geodesic paths in simulation spaces.

We note that the reduced basis method (RBM) [QMN16] can be understood as a spectral

method, where also a problem dependent approximation basis is used. In discussing the approximation properties of our method, we used a link to the spectral method and therefore expect a close relationship to the reduced basis method. Initial investigations for using the basis computed by our approach in an RBM-context do look promising.

Finally, the use of our approach in other industrial contexts is yet to be explored in detail. For example, we currently investigate the alignment of experimental measurement data in the form of point clouds from a real car crash in a crash facility with numerical simulation data. Here the aim is to find the corresponding numerical simulation to the measured point cloud data, for example to validate the numerical simulation approach or the involved material parameters. Such an alignment seemingly can be easier achieved in the eigenbasis obtained from the NICA operator.

Acknowledgements

The second author was partially supported by the Hausdorff Center for Mathematics in Bonn funded by the Deutsche Forschungsgemeinschaft. The authors were supported by the projects SIMDATA-NL and VAVID funded by the German Federal Ministry of Education and Research.

References

- [AGHH08] S. Ackermann, L. Gaul, M. Hanss, and T. Hambrecht. Principal component analysis for detection of globally important input parameters in nonlinear finite element analysis. *IAM Institute of Applied and Experimental Mechanics, Stuttgart*, 2008.
- [BBM14] M. Bauer, M. Bruveris, and P. W. Michor. Overview of the geometries of shape spaces and diffeomorphism groups. *J. Math. Imaging Vision*, 50(1-2):60–97, 2014.
- [BCG05] M. Ben-Chen and C. Gotsman. On the optimality of spectral compression of mesh data. *ACM Trans. Graph*, 24:60–80, 2005.
- [BGIT⁺13] B. Bohn, J. Garcke, R. Iza Teran, A. Paprotny, B. Peherstorfer, U. Schepsmeier, and C.-A. Thole. Analysis of car crash simulation data with nonlinear machine learning methods. In *Proceedings of the ICCS 2013*, pages 621–630. Elsevier, 2013.
- [BHM11] M. Bauer, P. Harms, and P. W. Michor. Sobolev metrics on shape space of surfaces. *Journal of Geometric Mechanics*, 3(4), 2011.
- [BN08] M. Belkin and P. Niyogi. Convergence of Laplacian eigenmaps. preprint, 2008.
- [BSW08] M. Belkin, J. Sun, and Y. Wang. Discrete Laplace operator on meshed surfaces. In *Proceedings of the Twenty-fourth Annual Symposium on Computational Geometry, SoCG '08*, pages 278–287. ACM, 2008.
- [Car83] E. Cartan. *Geometry of Riemannian Spaces*. Math Sci Press, 1983.
- [CL06] R. Coifman and S. Lafon. Diffusion maps. *Applied and Computational Harmonic Analysis*, 21(1):5–30, 2006.
- [Cos04] B. Costa. Spectral methods for partial differential equations. *CUBO A Mathematical Journal*, 6(4):1 – 32, 2004.
- [DJ94] D. L. Donoho and I. M. Johnstone. Ideal spatial adaptation by wavelet shrinkage. *Biometrika*, 81:425–455, 1994.

- [DRW10] T. K. Dey, P. Ranjan, and Y. Wang. Convergence, stability, and discrete approximation of Laplace spectra. In *Proceedings of the Twenty-first Annual ACM-SIAM Symposium on Discrete Algorithms*, SODA '10, pages 650–663, 2010.
- [FG09] C. Feuersänger and M. Griebel. Principal manifold learning by sparse grids. *Computing*, 85(4):267–299, 2009.
- [FJ07] P. T. Fletcher and S. Joshi. Riemannian geometry for the statistical analysis of diffusion tensor data. *Signal Processing*, 87:250–262, 2007.
- [GN13] D. Grebenkov and B. Nguyen. Geometrical structure of Laplacian eigenfunctions. *SIAM Review*, 55(4):601–667, 2013.
- [GSSV92] D. Gottlieb, C.-W. Shu, A. Solomonoff, and H. Vandeven. On the Gibbs phenomenon I: Recovering exponential accuracy from the Fourier partial sum of a nonperiodic analytic function. *Journal of Computational and Applied Mathematics*, 43(1–2):81–98, 1992.
- [GUKM08] D. Gomez-Ullate, N. Kamran, and R. Milson. An extended class of orthogonal polynomials defined by a Sturm-Liouville problem. *Journal of Mathematical Analysis and Applications*, 359(1):352–367, 2008.
- [HHM10] S. Huckemann, T. Hotz, and A. Munk. Intrinsic shape analysis: Geodesic PCA for Riemannian manifolds modulo isometric Lie group actions. *Statistica Sinica*, 20:1–100, 2010.
- [Iza14] R. Iza Teran. Enabling the analysis of finite element simulation bundles. *International Journal for Uncertainty Quantification*, 4(2):95–110, 2014.
- [JNT01] D. Jakobson, N. Nadirashvili, and J. Toth. Geometric properties of eigenfunctions. *Russian Math. Surveys*, 56:1085–1105, 2001.
- [KBCL99] D. G. Kendall, D. Barden, T. K. Carne, and H. Le. *Shape and Shape Theory*. Wiley, 1999.
- [KG00] Z. Karni and C. Gotsman. Spectral compression of mesh geometry. In *Proceedings of the 27th Annual Conference on Computer Graphics and Interactive Techniques*, SIGGRAPH '00, pages 279–286, 2000.
- [KHC12] D. Kushnir, A. Haddad, and R. Coifman. Anisotropic diffusion on sub-manifolds with application to earth structure classification. *Applied and Computational Harmonic Analysis*, 32(2):280–294, 2012.
- [LSLCO05] Y. Lipman, O. Sorkine, D. Levin, and D. Cohen-Or. Linear rotation-invariant coordinates for meshes. *ACM Trans. Graph.*, 24(3):479–487, 2005.
- [LSS⁺10] R. Lai, Y. Shi, K. Scheibel, S. Fears, R. Woods, A. Toga, and T. Chan. Metric-induced optimal embedding for intrinsic 3d shape analysis. In *Computer Vision and Pattern Recognition (CVPR), 2010 IEEE Conference on*, pages 2871–2878, 2010.
- [LV07] J. Lee and M. Verleysen. *Nonlinear Dimensionality Reduction*. Springer Publishing Company, Incorporated, 2007.
- [Mic08] P. Michor. *Topics in Differential Geometry*. American Mathematical Society, 2008.

- [MM06] P. W. Michor and D. Mumford. Riemannian geometries on spaces of plane curves. *J. Eur. Math. Soc.*, 8:1–48, 2006.
- [MMAC09] R. Myers, D. Montgomery, and C. Anderson-Cook. *Response Surface Methodology: Process and Product Optimization Using Designed Experiments*. WILEY, 2009.
- [MMP87] J. S. B. Mitchell, D. M. Mount, and C. H. Papadimitriou. The discrete geodesic problem. *SIAM J. Comput.*, 16(4):647–668, 1987.
- [Moh06] M.-J. Mohammad. *Special Functions: A Symmetric Generalization of Sturm-Liouville Problems and its Consequences*. Dissertation, University of Kassel, 2006.
- [MT08] L. Mei and C.-A. Thole. Data analysis for parallel car-crash simulation results and model optimization. *Sim. Modelling Practice and Theory*, 16(3):329–337, 2008.
- [OBCS⁺12] M. Ovsjanikov, M. Ben-Chen, J. Solomon, A. Butscher, and L. Guibas. Functional maps: A flexible representation of maps between shapes. *ACM Trans. Graph.*, 31(4):30:1–30:11, 2012.
- [QMN16] A. Quarteroni, A. Manzoni, and F. Negri. *Reduced Basis Methods for Partial Differential Equations*. Springer, 2016.
- [RBG⁺09] M. Reuter, S. Biasotti, D. Giorgi, G. Patanè, and M. Spagnuolo. Technical section: Discrete Laplace-Beltrami operators for shape analysis and segmentation. *Comput. Graph.*, 33(3):381–390, 2009.
- [RWP06] M. Reuter, F. Wolter, and N. Peinecke. Laplace-Beltrami spectra as ‘Shape-DNA’ of surfaces and solids. *Computer-Aided Design*, 38(4):342–366, 2006.
- [SC08] A. Singer and R. R. Coifman. Non-linear independent component analysis with diffusion maps. *Applied and Computational Harmonic Analysis*, 25(2):226–239, 2008.
- [Sin06] A. Singer. Spectral independent component analysis. *Applied and Computational Harmonic Analysis*, 21(2):135–144, 2006.
- [SJML05] A. Srivastava, S. Joshi, W. Mio, and X. Liu. Statistical shape analysis: Clustering, learning and testing. *IEEE Transactions on Pattern Analysis and Machine Intelligence*, 27:590–602, 2005.
- [StW13] A. Singer and H. tieng Wu. Spectral convergence of the connection Laplacian from random samples, 2013. arXiv/1306.1587.
- [Ter16] R. I. Teran. *Geometrical Methods for the Analysis of Simulation Bundles*. Dissertation, Universität Bonn, 2016. to be submitted.
- [TESK11] N. Thorstensen, P. Etyngier, F. Ségonne, and R. Keriven. Diffusion maps as a framework for shape modeling. *Comput. Vis. Image Underst.*, 115(4):520–530, 2011.
- [THJ13] T. D. Tran, J. Hofrichter, and J. Jost. An introduction to the mathematical structure of the Wright-Fisher model of population genetics. *Theory in Biosciences*, 132(2):73–82, 2013.
- [TNNC10] C. A. Thole, L. Nikitina, I. Nikitin, and T. Clees. Advanced mode analysis for crash simulation results. In *Proc. 9th LS-DYNA Forum*, 2010.
- [ZQZ11] P. Zhang, H. Qiao, and B. Zhang. An improved local tangent space alignment method for manifold learning. *Pattern Recognition Letters*, 32(2):181–189, 2011.